Spatially resolved horizontal spread in smouldering peat combining infrared and visual diagnostics

Hafiz M. F. Amin, Yuqi Hu and Guillermo Rein*

Department of Mechanical Engineering, Imperial College London, SW7 2AZ, UK

* Corresponding author. Email: g.rein@imperial.ac.uk; Tel: +44 (0) 20 7594 7036

Abstract

Smouldering wildfires in peatlands can last for weeks, resulting in the release of large amount of soil carbon and harmful emissions with detrimental effects on human health and the environment. Despite their importance, smouldering fires are poorly understood. An experimental study was carried out here to measure the spread rate of peat fire in detail, using infrared (IR) imaging. Peat samples with different moisture contents were prepared and burned in an open reactor of 20 x 20 cm^2 cross section and 10 cm depth, under laboratory-controlled conditions. In total, twelve experiments were studied, each lasting for 8 h on average. Infrared and visual cameras were synchronised, and images were acquired at a frequency of 1/min, for the duration of the experiment. Profiles of smouldering spread on the free surface of peat were tracked using an image intensity threshold and then used to calculate the horizontal spread rate. Temporally and spatially resolved spread rates are presented and analysed. Increasing the moisture content of the peat resulted in a decrease in spread rate and the smouldering front became increasingly irregular. At high moisture contents, spread at the lower layers of peat is faster compared to top surfaces which leads to formation of overhang, and IR is able to measure the formation of the overhang and its collapse as a step increase in horizontal spread. The overhang becomes more prominent when moisture content is increased. The new tool allows the study of unprecedented details in the spread of peat fires and can be adopted in future experimental studies.

Keywords: Infrared, smouldering, peat, moisture, wildfire

Please cite this article as:
Hafiz M.F. Amin, Yuqi Hu, and Guillermo Rein. "Spatially resolved horizontal spread in smouldering peat combining infrared and visual diagnostics." Combustion and Flame, vol 220 2020 328-336. https://doi.org/10.1016/j.combustflame.2020.06.039

Introduction

Peatlands store a large amount of organic carbon which is equivalent to about 70% of the entire carbon pool in the atmosphere [1]. Peatlands usually have high moisture contents (MCs) and thus rarely burn in wildfires. However, the drainage of peatlands due to human related activities and hot and dry weather perturbs hydrological feedbacks [2], and consequently lead to the drying of peat top layers and a decrease in water table. Prolonged dry spells put peatlands at a risk of fire [3, 4]. Heat released in a flaming wildfire can transfer to the organic rich soil, eventually igniting the peat and initiating a smouldering fire [5]. Once peat is ignited, it can burn slowly for weeks despite rains or firefighting attempts [5] because smouldering is the most persistent type of combustion [6]. Smouldering is controlled by heat losses and oxygen supply [7]. These fires are important due to the extent of damage they cause to the ecosystem and environment. For example, the 1997 El Nino smouldering megafire, which burnt throughout the forested peatlands of Indonesia, has been estimated to have burned 0.73 Mha of peatland and a release of carbon base emissions between 0.81 and 2.57 Gton [8].

In peatlands, MCs can vary to a large extent ranging from 10 to 300%, from drought to flood like conditions [9]. Several studies in the past have highlighted the importance of the moisture content (MC) in peat, demonstrating that it controls the ignition and spread rate of smouldering fires [10-14]. During smouldering process, drying is followed by an endothermic process of pyrolysis of the solid fuel and subsequently exothermic oxidation reactions [15]. Heat released during exothermic reactions partially radiates into the surrounding and partly heats the neighbouring fuel. If the heat released due to combustion is sufficient to overcome the heat loss to the surroundings, the smouldering front will move away from the ignition source and become self-sustained [7]. The smouldering front then propagates in the horizontal and downward directions [5, 6].

Please cite this article as:
Hafiz M.F. Amin, Yuqi Hu, and Guillermo Rein. "Spatially resolved horizontal spread in smouldering peat combining infrared and visual diagnostics." Combustion and Flame, vol 220 2020 328-336. https://doi.org/10.1016/j.combustflame.2020.06.039

Compared to flaming fires, smouldering dynamics are not well understood. Huang et al. [16] experimentally reported the lateral spread rate at varying conditions of moisture and wind. They measured temperature profiles at different locations in lateral and downward directions and reported the spread rates by analysing the temperature-time histories. Horizontal spread was found to decrease with MC. These spread rates were determined through the point measurements of temperature using thermocouples. Hu et al. [17] reported horizontal spread rates at different depths using thermocouple measurements. They found that spread rate decreases linearly with MC and horizontal spread became less sensitive to depths at higher MCs (> 25%). Non-uniform spread of the smouldering front cannot be considered through thermocouple measurement approach. Spread rates in the literature were resolved at point locations only for which a number of thermocouples were employed [17]. Infrared (IR) diagnostics have been used for continuous monitoring of smouldering experiments [16-20]. However, spread rates of smouldering along with collapse of overhang have not been previously investigated using thermal infrared imagery.

An important approach to study smouldering in field studies of peatlands is using infrared cameras due to larger scale of the spatial domain. Remote sensing of smouldering wildfires has attracted research interest to develop monitoring system using satellite data [21] or use of drones equipped with IR cameras. Compared to thermocouple measurements, infrared cameras offer the advantage of better spatial resolution and allow for a large burning area to be calculated.

In real peatlands, MCs, topography, inorganic contents and weather conditions, all have an influence on smouldering behaviour and can lead to inhomogeneous spread [22]. In this work, we alter the MC of peat and use thermal infrared and visual diagnostics to study the

Please cite this article as:
Hafiz M.F. Amin, Yuqi Hu, and Guillermo Rein. "Spatially resolved horizontal spread in smouldering peat combining infrared and visual diagnostics." Combustion and Flame, vol 220 2020 328-336. https://doi.org/10.1016/j.combustflame.2020.06.039

smouldering spread rate. An intensity threshold algorithm was developed to spatially and temporally resolved spread rates of smouldering by analysing the infrared images.

Experimental methods

The experimental setup used for the present study has been detailed in [23]. Only a brief description is given for the reader's convenience, and emphasis is put in the new IR diagnostics. A series of laboratory-controlled experiments were performed using an open-top reactor of 20 x 20 cm^2 cross section and 10 cm depth which is made of thick mineral wool board and is shown in Fig. 1 (a) [16, 17]. Peat samples of different MCs were burned in this reactor. A commercially available Irish sphagnum peat (Shamrock Irish Moss Peat, Bord na Mona Horticulture Ltd.), same as for previous studies, was used due to its consistent properties and homogenous compositions [16, 23]. Choice of this commercially available peat enables us to have repeatable and reliable experiments with least experimental uncertainty. The entire range of MCs, at which smouldering can self-sustain, was studied and peat samples with MCs on dry basis between 0 and 160 % were prepared. MC is defined as the mass of water divided by the mass of the dried peat [23]. It is difficult to the maintain the MC of the peat samples at exact values because biomass readily absorbs moisture available in the environment. The actual MC of peat samples were measured following the protocol detailed in [24] and were found to be 1.5 ± 0.9 % (dry peat); 26.7 ± 0.8 %; 54.5 ± 1.0 %; 78.2 ± 2.2 %; 103.0 ± 1.1 %; 125.4 ± 2.5 %; 142.9 ± 3.0 %; 158.7 ± 2.4 %. Peat samples were ignited by supplying 100 W power for 30 min to an ignition coil of 18 cm length, mounted 5 cm below the free surface. This ignition protocol has been used in other studies [16, 23] and has been reported to be strong enough to initiate self-sustained smouldering of peat having MCs of 160% [17]. The coil heats the peat locally and does not affect rest of the sample. To collect the emission from the smouldering of peat, an exhaust hood was placed above the reactor. Due to the physical constraint of the

Please cite this article as:
Hafiz M.F. Amin, Yuqi Hu, and Guillermo Rein. "Spatially resolved horizontal spread in smouldering peat combining infrared and visual diagnostics." Combustion and Flame, vol 220 2020 328-336. https://doi.org/10.1016/j.combustflame.2020.06.039

experimental setup, limited optical access was available and infrared radiations from the smouldering process were captured from the reflective surface using the infrared camera as shown in Fig. 1 (b). A Go-Pro camera was mounted inside the exhaust hood and acquired visual images of peat from the top of the reactor. Both infrared and visual image acquisition were synchronised with the start of power to ignition coil and images were captured at an interval of 1 min.

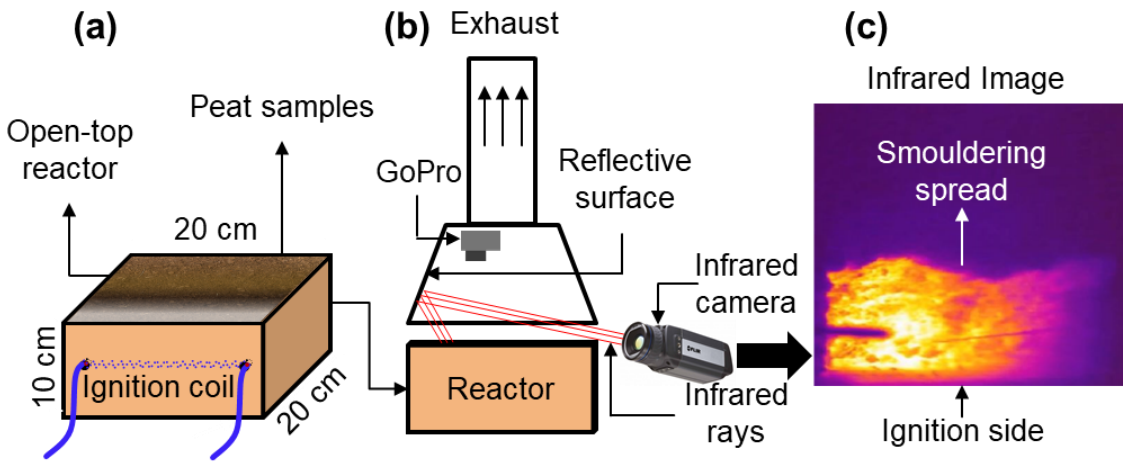


Fig. 1. Sketch of the open-top reactor (a), the infrared diagnostics applied to study smouldering of peat (b) and infrared image (c) of smouldering peat captured by infrared camera

In previous studies, the infrared camera had a view from above the reactor [16]. However, in this study, a ventilation system was placed on the top of the reactor which removed the emission plume continuously during the entire experimental time and it prevented accumulation of water vapour or smoke above the reactor. Camera viewing from the reflective surface resulted in the attenuation of some of radiation signal and required the distortion due to perspective to be corrected. Our camera (FLIR-A655sc) detects the infrared radiations between 7.5 to 14 µm. With such a broad detection wavelength, we have sufficient infrared signal in all experiments to detect the smouldering front. In addition, no quantitative data about radiation intensity is

Please cite this article as:
Hafiz M.F. Amin, Yuqi Hu, and Guillermo Rein. "Spatially resolved horizontal spread in smouldering peat combining infrared and visual diagnostics." Combustion and Flame, vol 220 2020 328-336. https://doi.org/10.1016/j.combustflame.2020.06.039

required for calculating the spread rates. Figure 2 (a) and (b) show the infrared images before and after applying the perspective correction, respectively. Unwanted pixels showing the boundary walls of reactor were removed from the image. The image correction was verified by comparing distance between points at opposite sides of the reactor and those were nearly same. Some small differences existed due to the slight deformation of the walls as can be seen in Fig 2 (b). The infrared data showed that peat started to burn near the ignition coil and the smouldering front propagates horizontally away from the ignition end. Infrared images were further analysed for calculating the spread rate at the surface of the smouldering peat. Smouldering fronts were tracked at every 15 min, using the intensity threshold algorithm. Smouldering has multiple fronts (drying, pyrolysis and oxidation fronts) [5, 6]. All three fronts have different temperature ranges and variation of infrared image intensities near the smouldering front is due to the different temperature ranges of the multi-front smouldering. Following the procedure of [25], a low threshold intensity value, which could correspond to drying region, was chosen and it was kept same during the entire set of experiments. Smouldering front is defined by the boundary at which the intensity exceeds the threshold. The first smouldering front at the top surface of peat was chosen when it moved away from the ignition side whereas the last smouldering front was chosen before it reached the opposite side of ignition end.

Please cite this article as:
Hafiz M.F. Amin, Yuqi Hu, and Guillermo Rein. "Spatially resolved horizontal spread in smouldering peat combining infrared and visual diagnostics." Combustion and Flame, vol 220 2020 328-336. https://doi.org/10.1016/j.combustflame.2020.06.039

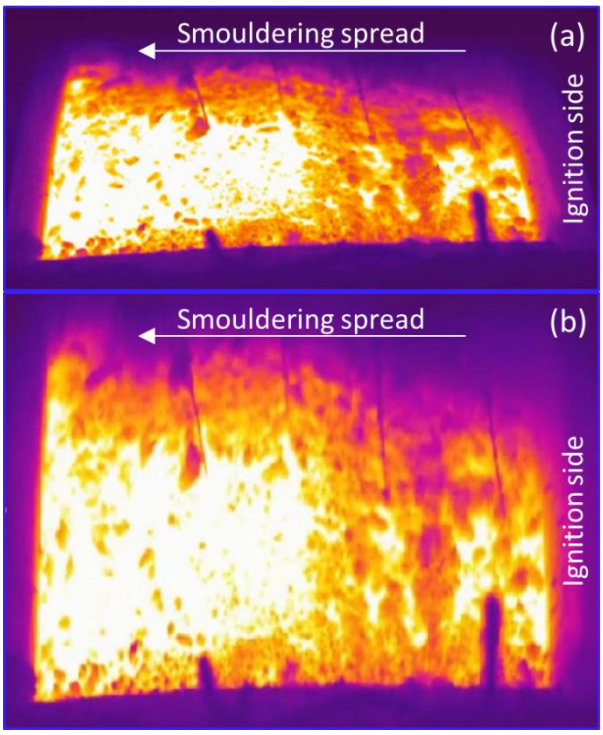
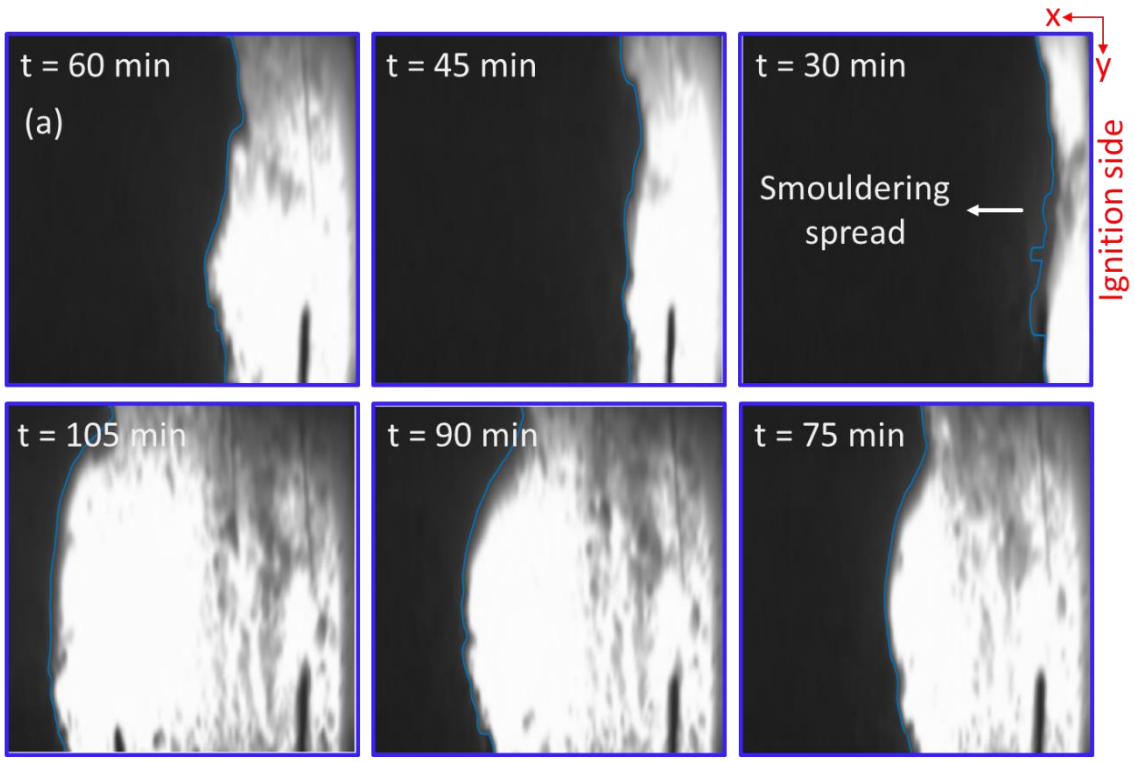


Fig. 2. Infrared image of smouldering peat in open top reactor (a) and infrared image after perspective view of the reactor is corrected (b). Peat has moisture content of 0%.



Please cite this article as:
Hafiz M.F. Amin, Yuqi Hu, and Guillermo Rein. "Spatially resolved horizontal spread in smouldering peat combining infrared and visual diagnostics." Combustion and Flame, vol 220 2020 328-336. https://doi.org/10.1016/j.combustflame.2020.06.039

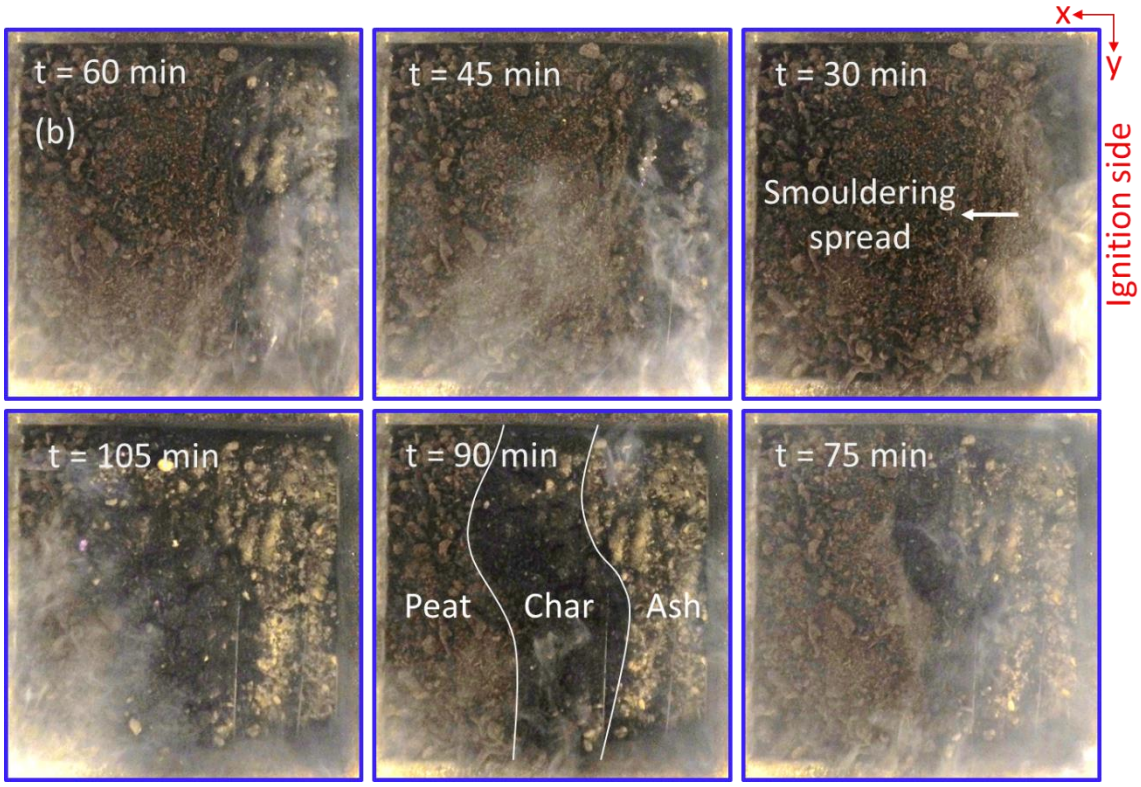


Fig. 3. Infrared images (a) showing the propagation of smouldering on the top surface of peat while visual diagnostic (b) shows the smouldering and the resulting smoke. White boundaries separating ash, char and peat can be seen in (b). These images are for dry peat.

Results and discussion

Smouldering fronts observed at the top surface of the reactor while burning dry peat are shown in Fig. 3. The first smouldering front is obtained 30 min after the ignitor started when the front moves away from the ignition side. Subsequently, the front was tracked every 15 min until it reaches the opposite side of the reactor at 105 min. A careful consideration of Fig. 3 reveals that the smouldering front does not propagate equally along the entire length (y-direction). These spread non-uniformities become more significant at higher MCs and are discussed in the next section. To average the non-uniformities, a linear fit was made. Figure 4 shows the smouldering front propagation in the horizontal direction and a linear fit made to smouldering profiles. The edge of the reactor wall near 10 cm was slightly distorted as can be seen in Fig.

Please cite this article as:
Hafiz M.F. Amin, Yuqi Hu, and Guillermo Rein. "Spatially resolved horizontal spread in smouldering peat combining infrared and visual diagnostics." Combustion and Flame, vol 220 2020 328-336. https://doi.org/10.1016/j.combustflame.2020.06.039

2(b) where the lower edge is not perfectly horizontal. During image correction, the distorted edge of the box hinders calculating the spread rate. Therefore, some pixels near y = 10 cm were not considered in spread rate calculations. Moreover, the choice to exclude the smouldering fronts touching the ignition end of the box and the opposite end, avoids biasing the linear fit of the propagation fronts. Spread rate in the horizontal direction (S) was calculated at the center of the reactor using the Eq. (1). t_{i+1} refers to the time 15 min after t_i.

$$s = \frac{x_{i+1} - x_i}{t_{i+1} - t_i} \quad (1)$$

Here x_i is the location of the fit to smouldering front at the center of reactor at time t_i.

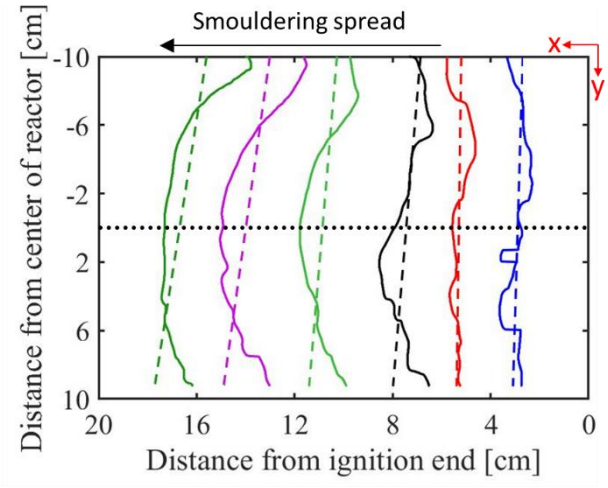


Fig. 4. Smouldering front propagation of dry peat in the horizontal direction. Dashed line shows a linear fit to the smouldering front and dotted lines in the middle shows the center of the reactor, where spread is measured.

Figure 5 shows the time (τ) it takes for the smouldering front at the top surface to leave the ignition end. These observations are possible due to spatially resolved IR data and are reported for the first time. Uncertainties along the ordinate are the number of images in which spread may have left the ignition end. Time (τ) to leave ignition end changes throughout the range of MC investigated here. For example, the time for the first front to leave the ignition end is 30

Please cite this article as:
Hafiz M.F. Amin, Yuqi Hu, and Guillermo Rein. "Spatially resolved horizontal spread in smouldering peat combining infrared and visual diagnostics." Combustion and Flame, vol 220 2020 328-336. https://doi.org/10.1016/j.combustflame.2020.06.039

min for the dry peat and it increases to 110 min when the MC is increased to 25%. At a MC of 160%, the time it takes for a smouldering front to leave the ignition end is 310 min which is of the order of the time it takes to reach the opposite end of the reactor. A linear fit is also overlaid on the plot which has an R^2 value of 0.8.

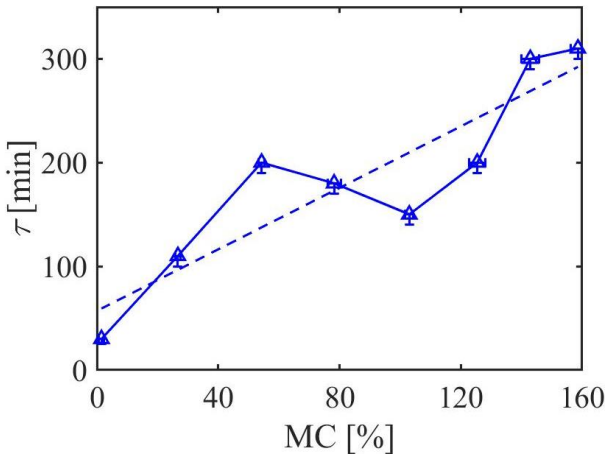


Fig. 5. Time (τ) for the first smouldering front to leave the ignition end at different MCs

Propagation of smouldering peat with different MCs are presented in Fig. 6, showing the spread rate at the center of the reactor versus the time since ignitor started. The shaded area shows the variation of spread rate along the entire smouldering front (y-direction) calculated between consecutive linear fits. Within each experiment, spread rate is not constant in the direction of spread at each MC and variations of spread rate increased with MC. Dry peat has been found to have the highest spread rate and its value varied between 9.6 and 13.7 [cm h^{-1}]. Increasing the MC from 0 to 160% leads to an 84% reduction of the spread rate.

Please cite this article as:
Hafiz M.F. Amin, Yuqi Hu, and Guillermo Rein. "Spatially resolved horizontal spread in smouldering peat combining infrared and visual diagnostics." Combustion and Flame, vol 220 2020 328-336. https://doi.org/10.1016/j.combustflame.2020.06.039

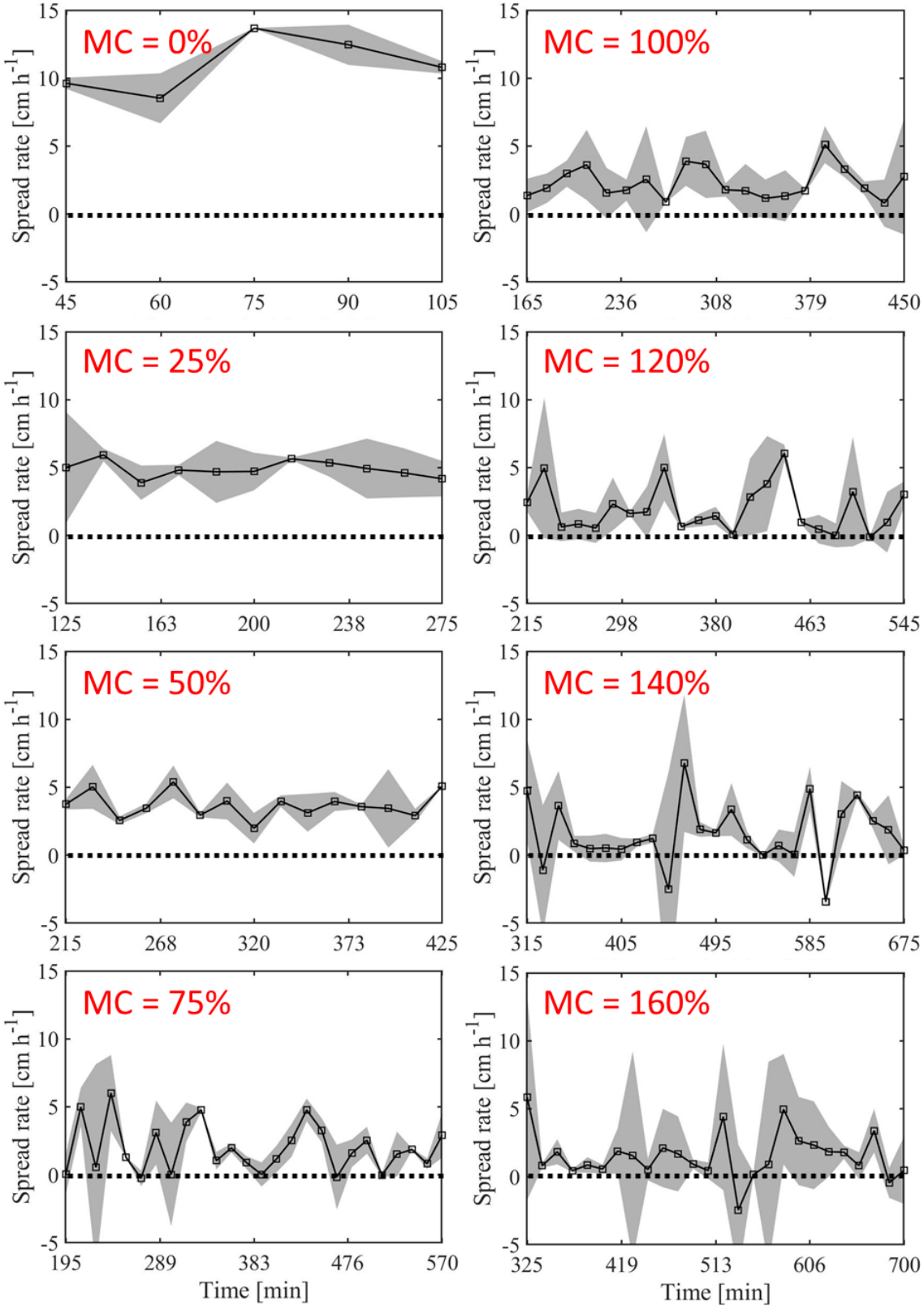


Fig. 6. Temporally resolved spread rate of smouldering at the top surface of peat calculated every 15 min after the smouldering front leaves the ignition side. The shaded area shows the

Please cite this article as:
Hafiz M.F. Amin, Yuqi Hu, and Guillermo Rein. "Spatially resolved horizontal spread in smouldering peat combining infrared and visual diagnostics." Combustion and Flame, vol 220 2020 328-336. https://doi.org/10.1016/j.combustflame.2020.06.039

range of spread rate variation calculated between consecutive linear fits. The dotted lines (in black) at zero value of spread rates are plotted for reference only.

It has been shown previously that increasing the MC above 50%, the spread at lower peat layers is higher compared to the top surface [16]. The difference in spread rate at the top and lower surfaces leads to the formation of overhang as shown in Fig. 7 and was first reported in [16]. Due to the horizontal spread (x-direction) underneath the top surface, overhang length increases and the char under the top surface is unable to support the temporary hanging surface of smouldering peat which eventually collapses.

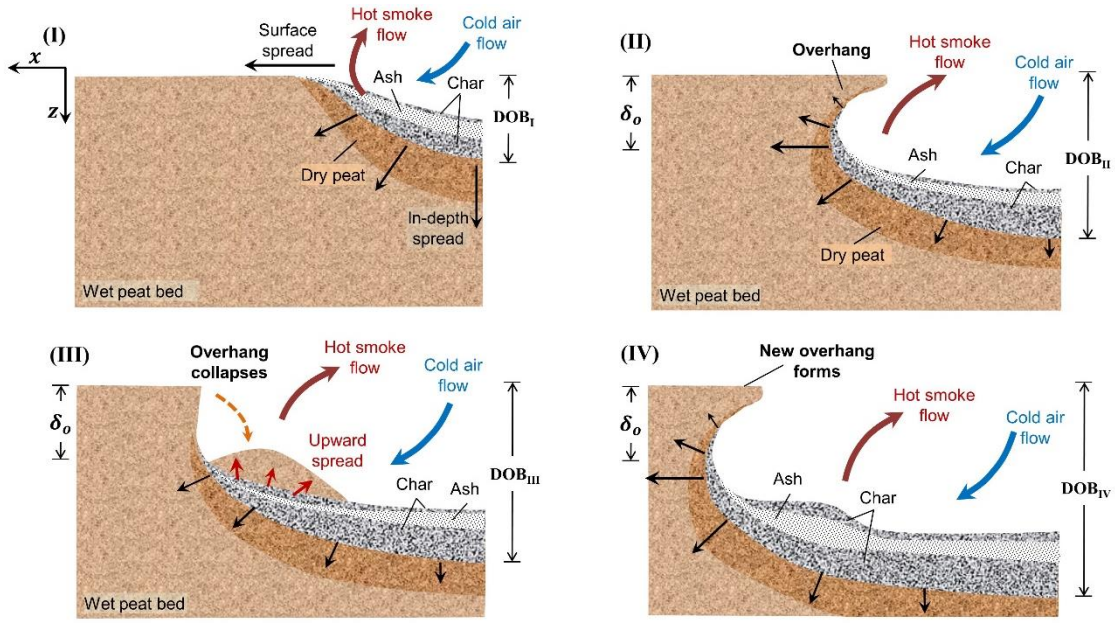


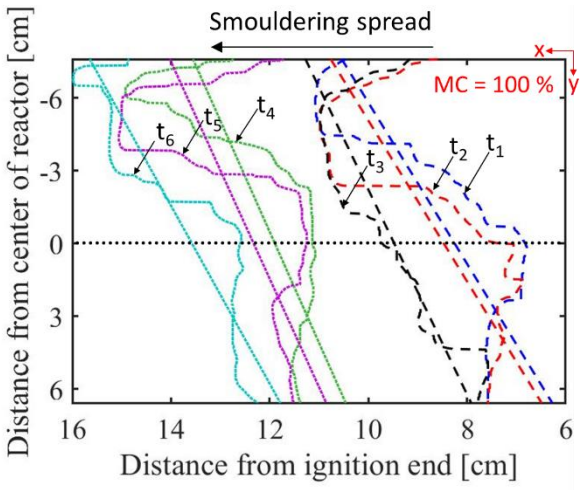
Fig. 7. Schematic diagram for the periodic formation and collapse of overhang in smouldering spread over wet peat: (I) soon after ignition, (II) formation of the overhang, (III) collapse and consumption of the overhang, and (IV) formation of a new overhang. Illustration from [16] (X. Huang, CC BY license)

As the MC of the peat increases beyond 50%, the top surface of peat does not entirely degrade into char due to the lower temperatures [17]. In this work, at MC more than 50%, we have

Please cite this article as:
Hafiz M.F. Amin, Yuqi Hu, and Guillermo Rein. "Spatially resolved horizontal spread in smouldering peat combining infrared and visual diagnostics." Combustion and Flame, vol 220 2020 328-336. https://doi.org/10.1016/j.combustflame.2020.06.039

tracked the collapse of top surface due to overhang which is represented by a sudden increase in spread rate and is discussed further under the discussion of Fig. 9. Tracking collapse of overhang gave us the smouldering spread rate at lower surfaces.

Figure 8 shows smouldering profiles at various locations in sample with 100% MC. To keep the visibility of the plot clear and to explain the observation of the collapse of overhang, only two collapse events are shown. Irregularities of the profiles along y-direction are more prominent at MC = 100 %. Local conditions of density, particle size, porosity, wind and MC can be non-uniform. Despite our efforts to produce homogeneous samples, all these factors contribute to irregular smouldering front. Three consecutive smouldering profiles are marked with t_1, t_2 and t_3 and their fits are shown with dashed lines. Another set of three smouldering profiles is marked with t_4, t_5 and t_6 and their linear fit is shown with dotted lines. The distance between t_1 and t_2 profiles is less than the distance between the t_2 and t_3 profiles which is also clear from their linear fits. The same is true for dotted lines t_4, t_5 and t_6. An increased shift of t_3 from t_2 profiles compared to shift of t_2 from t_1 in same interval of time (15 min) is due to the collapse of overhang.



Please cite this article as:
Hafiz M.F. Amin, Yuqi Hu, and Guillermo Rein. "Spatially resolved horizontal spread in smouldering peat combining infrared and visual diagnostics." Combustion and Flame, vol 220 2020 328-336. https://doi.org/10.1016/j.combustflame.2020.06.039

Fig. 8. Smouldering front propagation in the horizontal direction at MC = 100%. A linear fit to the smouldering front is also shown. t_1 to t_3 and t_4, to t_6 show collapse of overhang at two different locations.

One of the advantages of using IR diagnostic is that the spread rates can be resolved spatially, which allows us to study the collapse of overhang at higher MCs. Figure 9 shows plots of horizontal spread vs. distance from ignition location for different MCs. The error bars show the uncertainties in measurements due to uncertainties in location of smouldering fronts. Dashed lines show average spread rate calculated between the first and last front positions. The first smouldering rate reported at a MC of 0% is at a location of 5.3 cm which is the location of second smouldering tracked in horizontal direction. The last smouldering spread rate is reported at the location of 16.7 cm away from ignition end. After this location, part of smouldering front reaches the opposite side of the ignition end in the next 15 min and no further spread rate is reported beyond this location. Increasing the MC beyond 75% leads to a fluctuation in spread rate. This is because the top surface of peat is not burning, but the observed spread in IR is the result of overhang and collapse phenomenon [16]. This can be seen for high MC where a large increase in the spread rate is associated with a jump in location of the front. For example, at a MC of 120%, peak values of propagation front (shown in circles) follow a relatively large shift in the location of propagation front from their preceding ones. At MC of 140 and 160 %, negative spread rates (shown in squares) are also reported. Negative spread means that the propagation front has shifted back due to the collapse of overhang. After the collapse of the overhang, the spread rate sharply increases when the collapsed peat layer gets heated by absorbing heat from its lower layers of smouldering peat.

Experiments at 50 and 100% MC were repeated three times. Figure 10 shows the spread of smouldering at MC of 50 % and 100 %. The shaded area shows the range of spread rate

Please cite this article as:
Hafiz M.F. Amin, Yuqi Hu, and Guillermo Rein. "Spatially resolved horizontal spread in smouldering peat combining infrared and visual diagnostics." Combustion and Flame, vol 220 2020 328-336. https://doi.org/10.1016/j.combustflame.2020.06.039

calculated from a set of three experiments at the center of reactor. For smouldering in peat with MC of 50%, smouldering spread rate can vary up to 40 % from the mean during the repeat of experiments at same conditions. However, at MC of 100%, the propagation rates at the top surface can vary significantly between experiments. Maximum variation of propagation rate is found to be 110% different from the mean. This is due to different timings of collapse of an overhang during different experiments but with similar conditions.

Please cite this article as:
Hafiz M.F. Amin, Yuqi Hu, and Guillermo Rein. "Spatially resolved horizontal spread in smouldering peat combining infrared and visual diagnostics." Combustion and Flame, vol 220 2020 328-336. https://doi.org/10.1016/j.combustflame.2020.06.039

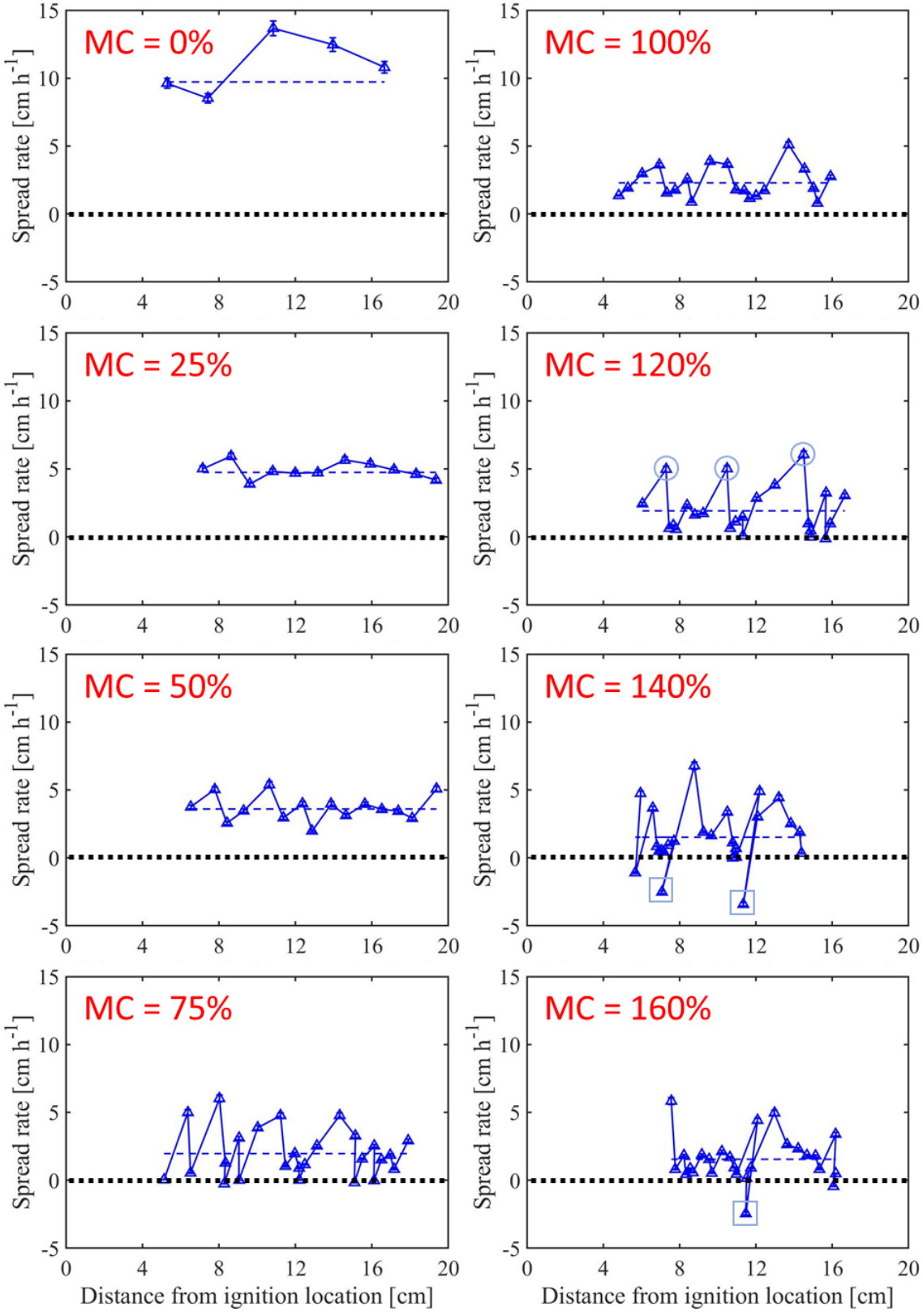


Fig. 9. Spatially resolved spread rate of smouldering at the top surface of peat calculated every 15 min after the smouldering front leaves the ignition side. In some of the plots error

Please cite this article as:
Hafiz M.F. Amin, Yuqi Hu, and Guillermo Rein. "Spatially resolved horizontal spread in smouldering peat combining infrared and visual diagnostics." Combustion and Flame, vol 220 2020 328-336. https://doi.org/10.1016/j.combustflame.2020.06.039

bars are smaller than the marker size. Dashed line shows average spread rate calculated between the first and last smouldering front. The dotted lines (in black) at zero value of spread rates are plotted for reference only.

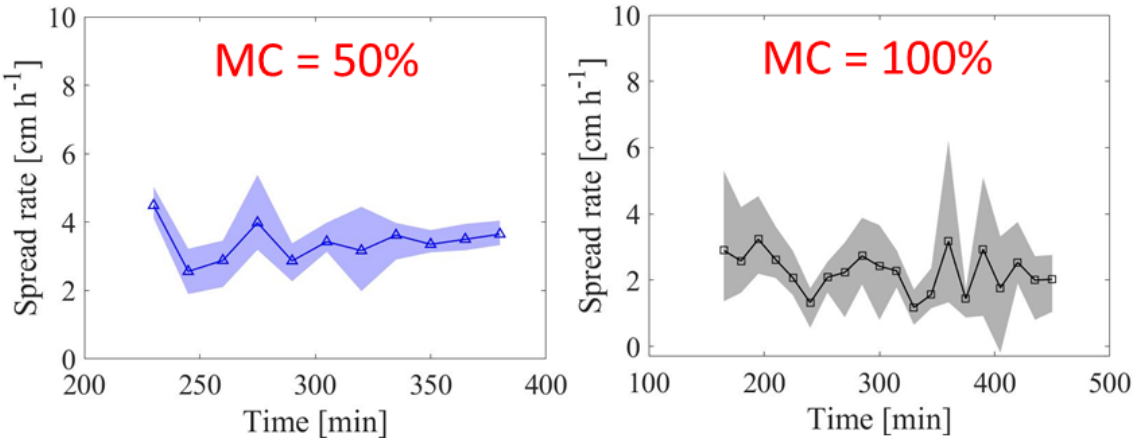


Fig. 10. Spatially resolved spread rate of smouldering at the top surface of peat from repeated experiments at MC of 50% and 100%. Shaded area shows the range of spread rate calculated from a set of three experiments at the center of the reactor.

Figure 11 shows the average spread rates calculated using infrared images in this study at different MCs. Recently reported horizontal spread rate of smouldering at different layers of peat of varying MC are also overlaid in this figure [17]. Hu et al.[17], calculated smouldering spread rates from thermocouple measurements at the middle of the reactor. At MCs <50%, smouldering spread rates measured by infrared at the top surface of peat are lower than the smouldering spread reported by thermocouple measurements. This could be because the spread rate calculated from thermocouples shows the values from point measurements whereas the IR imaging takes into account inhomogeneities of the propagation of smouldering front by making a linear fit. At MCs > 25%, the smouldering spread rates reported by [17] at 8 cm depth matches well with the propagation rates at the surface of the peat calculated here using infrared measurements. Moreover, in [17], it is reported that smouldering spread rates remain insensitive to the depth at higher MCs. These conclusions suggest that it is reasonable to

Please cite this article as:
Hafiz M.F. Amin, Yuqi Hu, and Guillermo Rein. "Spatially resolved horizontal spread in smouldering peat combining infrared and visual diagnostics." Combustion and Flame, vol 220 2020 328-336. https://doi.org/10.1016/j.combustflame.2020.06.039

assume that the average surface propagation at the top surface is same at the smouldering spread rate in the deep layers for these experiments.

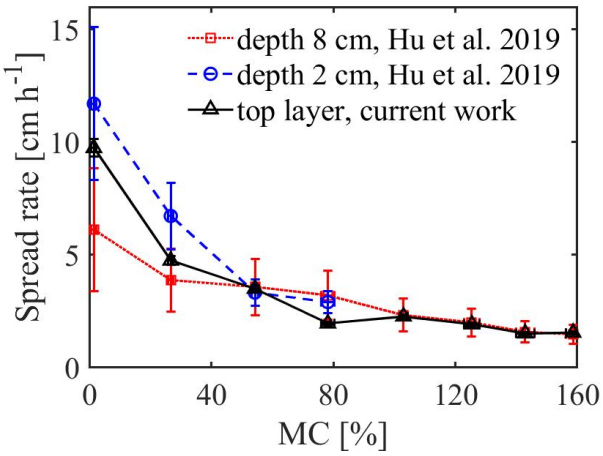


Fig. 11. Average spread rate of smouldering at the top surface of peat at different MC. Data points marked with 'circle' and 'square' are reported in [17] whereas the 'triangle' shows the measurements of current work.

Conclusions

Infrared analysis of laboratory-controlled experiments was carried out to investigate the smouldering propagation in peat samples. IR analysis allowed us to report the shape of smouldering fronts and temporally and spatially resolved spread rates which is not possible with other diagnostics such thermocouple measurement and visual images. Irregularities in the smouldering fronts were found to increase with moisture content and were taken into account by making a linear fit to the spreading profiles. Through IR diagnostics, it was observed that the time it takes for smouldering front to leave ignition end also changes over a range of MC studied here. The spread rate of smouldering was found to decrease with MC. At MCs greater than 50%, tracking the collapse of overhang gave us the smouldering spread rate at deep layers. The size of overhang length varied and where the overhang length was large, collapse resulted in larger spread rates and a larger shift of the spread in the horizontal direction. Average spread

Please cite this article as:
Hafiz M.F. Amin, Yuqi Hu, and Guillermo Rein. "Spatially resolved horizontal spread in smouldering peat combining infrared and visual diagnostics." Combustion and Flame, vol 220 2020 328-336. https://doi.org/10.1016/j.combustflame.2020.06.039

rate in each experiment was also reported which showed an overall good agreement with previously reported spread rates using thermocouples. IR measurements improve the study of peat fire providing unprecedented details not observed before.

Acknowledgements

The research has been funded by the European Research Council (ERC) Consolidator Grant HAZE (682587). Authors would like to thank Eirik Christensen and Muhammad A. Santoso from Imperial Hazelab for their time for helpful discussion.

References

[1] M. Parry, M.L. Parry, O. Canziani, J. Palutikof, P. Van der Linden, C. Hanson, Climate change 2007-impacts, adaptation and vulnerability: Working group II contribution to the fourth assessment report of the IPCC, Cambridge University Press2007. doi: https://doi.org/10.2134/jeq2008.0015br.

[2] J. Waddington, P. Morris, N. Kettridge, G. Granath, D. Thompson, P. Moore, Hydrological feedbacks in northern peatlands, Ecohydrology 8 (2015) 113-127. doi: https://doi.org/10.1002/eco.1493.

[3] M. Turetsky, W. Donahue, B. Benscoter, Experimental drying intensifies burning and carbon losses in a northern peatland, Nat Commun 2 (2011) 514. doi: https://doi.org/10.1038/ncomms1523.

[4] M.R. Turetsky, B. Benscoter, S. Page, G. Rein, G.R. Van Der Werf, A. Watts, Global vulnerability of peatlands to fire and carbon loss, Nat Geosci 8 (2015) 11. doi: https://doi.org/10.1038/ngeo2325.

[5] G. Rein, Smouldering fires and natural fuels Fire phenomena and the Earth system: an interdisciplinary guide to fire science'.(Ed. CM Belcher) pp, (2013) 15-33. doi: https://doi.org/10.1002/9781118529539.ch2.

[6] G. Rein, Smoldering combustion, SFPE Handbook of Fire Protection Engineering, Springer 2016, pp. 581-603. doi: https://doi.org/10.1007/978-1-4939-2565-0_19

[7] T.J. Ohlemiller, Modeling of smoldering combustion propagation, Prog Energy Combust Sci 11 (1985) 277-310. doi: https://doi.org/10.1016/0360-1285(85)90004-8.

[8] S.E. Page, F. Siegert, J. Rieley, H.-D. Boehm, V., Jaya, A., and Limin, S.: 2002,'The amount of carbon released from peat and forest fires in Indonesia during 1997', Nature 420 (2002) 61-65. doi: https://doi.org/10.1038/nature01131.

[9] L. Moreno, M.-E. Jiménez, H. Aguilera, P. Jiménez, A. de la Losa, The 2009 smouldering peat fire in las tablas de daimiel national park (Spain), Fire Technol 47 (2011) 519-538. doi: https://doi.org/10.1007/s10694-010-0172-y.

[10] W.H. Frandsen, The influence of moisture and mineral soil on the combustion limits of smoldering forest duff, Can. J. For. Res. 17 (1987) 1540-1544. doi: https://doi.org/10.1139/x87-236.

[11] X. Huang, G. Rein, Smouldering combustion of peat in wildfires: Inverse modelling of the drying and the thermal and oxidative decomposition kinetics, Combust Flame 161 (2014) 1633-1644. doi: https://doi.org/10.1016/j.combustflame.2013.12.013.

[12] X. Huang, G. Rein, Computational study of critical moisture and depth of burn in peat fires, Int J Wildland Fire 24 (2015) 798-808. doi: https://doi.org/10.1071/WF14178.

[13] B. Lawson, W. Frandsen, B. Hawkes, G. Dalrymple, Probability of sustained smoldering ignition for some boreal forest duff types, (1997).

[14] J. Reardon, R. Hungerford, K. Ryan, Factors affecting sustained smouldering in organic soils from pocosin and pond pine woodland wetlands, Int J Wildland Fire 16 (2007) 107-118. doi: https://doi.org/10.1071/WF06005.

Please cite this article as:
Hafiz M.F. Amin, Yuqi Hu, and Guillermo Rein. "Spatially resolved horizontal spread in smouldering peat combining infrared and visual diagnostics." Combustion and Flame, vol 220 2020 328-336. https://doi.org/10.1016/j.combustflame.2020.06.039

[15] R.M. Hadden, G. Rein, C.M. Belcher, Study of the competing chemical reactions in the initiation and spread of smouldering combustion in peat, Proc Combust Inst 34 (2013) 2547-2553. doi: https://doi.org/10.1016/j.proci.2012.05.060.

[16] X. Huang, F. Restuccia, M. Gramola, G. Rein, Experimental study of the formation and collapse of an overhang in the lateral spread of smouldering peat fires, Combust Flame 168 (2016) 393-402. doi: https://doi.org/10.1016/j.combustflame.2016.01.017.

[17] Y. Hu, E.G. Christensen, H.M.F. Amin, T.E.L. Smith, G. Rein, Experimental study of moisture content effects on the transient gas and particle emissions from peat fires, Combust Flame, (2019). doi: https://doi.org/10.1016/j.combustflame.2019.07.046.

[18] E. Pastor, I. Oliveras, E. Urquiaga-Flores, J.A. Quintano-Loayza, M. Manta, E. Planas, A new method for performing smouldering combustion field experiments in peatlands and rich-organic soils, Int J Wildland Fire 26 (2018) 1040-1052. doi: https://doi.org/10.1071/WF17033.

[19] C. Burke, S. Wich, K. Kusin, O. McAree, M.E. Harrison, B. Ripoll, Y. Ermiasi, M. Mulero-Pázmány, S. Longmore, Thermal-Drones as a Safe and Reliable Method for Detecting Subterranean Peat Fires, Drones 3 (2019) 23. doi: https://doi.org/10.3390/drones3010023.

[20] N. Prat-Guitart, G. Rein, R.M. Hadden, C.M. Belcher, J.M. Yearsley, Effects of spatial heterogeneity in moisture content on the horizontal spread of peat fires, Sci. Total Environ. 572 (2016) 1422-1430. doi: https://doi.org/10.1016/j.scitotenv.2016.02.145.

[21] P. Sofan, D. Bruce, E. Jones, J. Marsden, Detection and Validation of Tropical Peatland Flaming and Smouldering Using Landsat-8 SWIR and TIRS Bands, Remote Sens. 11 (2019) 465. doi: https://doi.org/10.3390/rs11040465.

[22] N. Prat-Guitart, C.M. Belcher, D.K. Thompson, P. Burns, J.M. Yearsley, Fine-scale distribution of moisture in the surface of a degraded blanket bog and its effects on the potential spread of smouldering fire, Ecohydrology 10 (2017) e1898. doi: https://doi.org/10.1002/eco.1898

Please cite this article as:
Hafiz M.F. Amin, Yuqi Hu, and Guillermo Rein. "Spatially resolved horizontal spread in smouldering peat combining infrared and visual diagnostics." Combustion and Flame, vol 220 2020 328-336. https://doi.org/10.1016/j.combustflame.2020.06.039

[23] Y. Hu, E. Christensen, F. Restuccia, G. Rein, Transient gas and particle emissions from smouldering combustion of peat, Proc Combust Inst 37 (2019) 4035-4042. doi: https://doi.org/10.1016/j.proci.2018.06.008.

[24] E. Christensen, Y. Hu, F. Restuccia, M.A. Santoso, X. Huang, G. Rein, Experimental methods and scales in smouldering wildfires, in: A.C. Paulo Pereira, J. Mataix-Solera, X. Ubeda, G. Rein (Eds.) Fire Effects on Soil Properties CSIRO Publishing 2019 pp. 267-280. Chapter 17, doi: https://doi.org/10.1071/9781486308149.

[25] E.G. Christensen, N. Fernandez-Anez, G. Rein, Influence of soil conditions on the multidimensional spread of smouldering combustion in shallow layers, Combust Flame 214 (2020) 361-370. doi: https://doi.org/10.1016/j.combustflame.2019.11.001.

Please cite this article as:
Hafiz M.F. Amin, Yuqi Hu, and Guillermo Rein. "Spatially resolved horizontal spread in smouldering peat combining infrared and visual diagnostics." Combustion and Flame, vol 220 2020 328-336. https://doi.org/10.1016/j.combustflame.2020.06.039